500-Year Eccentric Orbits for the Cassini Spacecraft within the Saturnian System

Chris Patterson,[*] Masaki Kakoi,[*] Kathleen Howell,[†] Chit Hong Yam,[*] and James M. Longuski[‡]

One option for efficient and safe disposal of the Cassini spacecraft includes eccentric, long-term orbits between the Saturnian moons that allow for continued observations of the Saturnian system for an extended period of time. The focus of the current effort is the determination of an eccentric orbit about Saturn with periapsis above Titan. Determination of a configuration of this type, sustained under all relevant gravitational perturbations for 500 years or more with no collisions, presents a significant challenge. In addition, insertion into such an orbit must be accomplished via Titan encounters and with limited maneuver capability.

INTRODUCTION

The Cassini mission continues to generate impressive results. However, the final options for the Cassini spacecraft must ultimately be decided and a controlled end-of-life mission scenario selected. Previous missions to the planets have concluded in various ways, such as spacecraft planetary impact and extended missions involving escape of the spacecraft from the planetary system. The Pioneer 10 and 11 spacecraft as well as the Voyager I and II missions were designed for flybys of the outer planets and, once the missions were complete, they escaped the solar system entirely [1,2]. In contrast, the Galileo mission was designed to orbit its target planet, Jupiter, and ended with a Jupiter impact in 2003 [3]. Similarly, Magellan, in orbit about Venus for over 4 years, was eventually lowered into the Venus atmosphere at the end of its mission. As an alternative to planetary impact, the Mars orbiters, Mariner 9 [4], as well as Vikings I and II [5] were all placed in higher, long-term orbits before being shut down to limit contamination of Mars.

For the Cassini mission, a wide range of options are being considered for an end-of-life scenario. The spacecraft may impact on Saturn [6], remain in the Saturnian system, or escape to a heliocentric trajectory. Once escaped, a large heliocentric orbit is an option [7] or the vehicle can be delivered to one of the other outer planets [8]. If the spacecraft remains in orbit about Saturn without impact, the potential trajectories can be investigated in terms of two regions. The orbit can be designed to remain beyond the orbit of Phoebe [7]; alternatively, a smaller orbit closer to Saturn is possible, most likely a long-term eccentric orbit between Titan and Phoebe. The study here examines this latter option in detail. Any such orbit potentially enhances future observations of Saturn and its environs for an extended time. The design of such orbits is constrained by the requirement to avoid collisions with any moons, particularly Titan. Thus, these orbits must be accessible from the current Cassini trajectory and maintain their characteristics over long-term propagation under gravitational perturbations of the Sun, Jupiter, Titan, and other moons of Saturn. The objective, then, is the determination of the characteristics of an orbit about Saturn with periapsis above Titan, such that the orbit remains in a stable configuration under all relevant gravitational perturbations for at least 500 years with no collisions.

[*] Ph.D. Student, School of Aeronautics and Astronautics, Purdue University, Neil Armstrong Hall of Engineering, 701 W. Stadium Ave., West Lafayette, Indiana 47907-2045; Student Member AIAA.
[†] Hsu Lo Professor of Aeronautical and Astronautical Engineering, School of Aeronautics and Astronautics, Purdue University, Neil Armstrong Hall of Engineering, 701 W. Stadium Ave., West Lafayette, Indiana 47907-2045; Fellow AAS; Associate Fellow AIAA.
[‡] Professor of Aeronautical and Astronautical Engineering, School of Aeronautics and Astronautics, Purdue University, Neil Armstrong Hall of Engineering, 701 W. Stadium Ave., West Lafayette, Indiana 47907-2045; Member AAS; Associate Fellow AIAA.

BACKGROUND

Regime between Titan and Phoebe

The Saturnian trajectories considered here are large, eccentric orbits with periapses above the orbit of Titan. As such, they are generally considered to be irregular. Among the orbits of naturally occurring satellites or moons in the solar system, there is a distinct classification of two general types: regular and irregular. An understanding of irregular orbits in the region between Titan and the distant moon Phoebe places the options under consideration in some context.

Regular orbits are relatively small, nearly circular, and usually possess low inclinations with respect to the planet's equator. In contrast, irregular orbits are larger and are characterized by higher eccentricities and, sometimes, high inclinations with respect to the planet's equator. Among the natural satellites, it is also true that the regular orbits are always prograde while the irregulars are often retrograde. In comparing regular to irregular satellite orbits, size is often related to the Hill sphere radius, that is,

$$r_H = a_p \left[\frac{M_p}{3M_\odot} \right]^{1/3} \tag{1}$$

where M_p is the mass of the planet, a_p is planet semimajor axis, and $M_\odot$ is the mass of the Sun. Equation (1) also serves as the first term in an expansion for the range between a planet and either of the nearest collinear libration points in the Sun-planet system [9], thus, it approximates this distance well. The radius of the Hill sphere around Saturn is 6.518×10^7 km or 1081 R_S (Saturn radii,) while the distance from Saturn to the Sun-Saturn L_1 libration point is 6.417×10^7 km (1064 R_S) and the distance to L_2, on the opposite side of Saturn, is 6.615×10^7 km (1098 R_S). Satellites in regular orbits typically possess a semi-major axis with a value that is less than 0.05 r_H. All known irregular satellites in prograde orbits are described in terms of semi-major axes that range between 0.05 r_H and 0.33 r_H, with apoapse radii no greater than 0.47 r_H. Irregular satellites in retrograde orbits are typically characterized by semi-major axes within 0.47 r_H and apoapse radii that extend to 0.65 r_H [10]. This is consistent with analytical and numerical results by Hamilton and Krivov [11]. The irregular orbits of natural satellites are also bound by limits on inclination, that is, $i \leq 55^o$ (or $\geq 130^o$ in the cases of retrogrades) with respect to the planet's orbital plane [12]. Beyond these limits on orbit size and shape, solar perturbations cause the orbit to escape on long time scales.

In the Saturnian system, Iapetus is sometimes considered to be in an irregular orbit [10]. The semi-major axis is 0.056 r_H, eccentricity is equal to 0.0269, with an inclination equal to 7^o. All of these values are high for a regular satellite, but low for an irregular. In contrast, Phoebe is certainly in an irregular orbit. Phoebe's orbit is retrograde, the apoapse distance is 0.217 r_H, the eccentricity value is 0.163 and the inclination is 176^o.

The objective for this investigation is a design strategy in a regime between Titan and Phoebe. The orbits of interest are large, eccentric, and prograde. Thus, the target orbits qualify as irregulars by the above definitions. For this analysis, it is assumed that the spacecraft will remain in the vicinity of Saturn for as long as possible, potentially expanding science opportunities given that the spacecraft systems remain operational. It is also required that the spacecraft avoid escaping Saturn on any uncontrolled trajectory that may intersect other solar system bodies, particularly the inner planets, for at least the first 500 years. Thus, the orbit must satisfy the stability requirement consistent with prograde irregulars, i.e., its apoapsis should not exceed $0.47 r_H$; such a constraint will lower the risk of escape.

Given the existence of an orbit that satisfies the requirements, it must be accessible from a likely trajectory for the Cassini spacecraft near the end of the mission and within the available ΔV limits. Because of these constraints, the delivery and final long-term orbits are designed simultaneously. The process to enter into the long-term orbits begins with a series of Titan flybys in a patched-conic model. These Titan encounters pump up the size of the orbit until it is sufficiently large such that the periapse-raise maneuver is within the ΔV budget. The flybys can also be designed to yield a final orbit with specific geometric

requirements. A maneuver is then applied at apoapsis (within one year of the final Titan flyby) to raise the periapse radius above Titan's orbit. Once periapsis above Titan is achieved, the trajectory is propagated for 500 years in a model including the gravitational effects of the Sun, Saturn, Titan, Hyperion, Iapetus, Phoebe, and Jupiter in a true ephemeris model using the JPL de408 and sat242l data. The possibility of an impact with Titan, or any other moon of Saturn within the first 500 years is considered. The orbit variations due to solar gravity perturbations alone can be significant, particularly for an orbit with low inclination relative to the Saturn ecliptic plane. The goal in examining the orbit variations is, initially, to determine if periapsis will be reduced to a distance that allows for future Titan encounters. Then, to determine the basis of a design strategy, the long-term variation in the periapse distance is examined in response to modifications in the post-encounter orbit. The effects of solar perturbations on periapsis can be mitigated by particular orbit geometry such that periapsis does not fall below Titan's orbit within the 500-year time interval.

Trajectory Requirements

Insertion into a long-term orbit about Saturn from a pre-determined initial state must be accomplished via Titan encounters and with only limited ΔV capability. This end-of-life investigation naturally originates from a spacecraft state at the end of the extended mission. Thus, in general, sets of end conditions for the extended mission are assumed as the potential initial states for the end-of-life mission. In examining two sample states, these conditions include either V_∞ = 5.49 km/s or V_∞ = 5.887 km/s with respect to Titan.

For the purposes of this work, it is desirable for the end-of-life scenario to use less than 50 m/s ΔV, but a maximum of 100 m/s is assumed to be available. The expectation of a limited spacecraft hardware lifespan also imposes constraints on the time-of-flight allowed between the final Titan encounter and the final spacecraft maneuver. Specifically, the last spacecraft maneuver should not occur more than one year after the final Titan flyby.

Conic Analysis: Requirements for an Optimal Periapsis Raise

Assume that the spacecraft is orbiting Saturn with an apoapse radius equal to r_a and a periapse radius $r_{p,old}$. Then, the ΔV cost (applied at apoapsis) to raise the periapsis to a target value, $r_{p,new}$, is

$$\Delta V = \sqrt{2\mu\left[1/r_a - 1/(r_a + r_{p,new})\right]} - \sqrt{2\mu\left[1/r_a - 1/(r_a + r_{p,old})\right]} \tag{2}$$

where μ is the gravitational parameter of Saturn. Clearly, from Equation (2), if the orbital period and the target periapsis are given (i.e., r_a and $r_{p,new}$ are known), then the ΔV cost of a periapse-raise maneuver decreases with a larger pre-maneuver periapsis radius, $r_{p,old}$. Consider a series of resonant Titan flybys designed to increase periapsis to its maximum value before adding a maneuver to raise it further to the target value; assume a constant V_∞ = 5.490 km/s at each Titan encounter. The Saturn-Titan distance is then the largest periapsis value that the spacecraft can achieve via such Titan flybys. In this scenario, the final Titan flyby occurs at the spacecraft periapsis with respect to Saturn. When the flyby of the moon occurs at an apse of the spacecraft orbit, the spacecraft orbit will simultaneously reach maximum inclination with respect to the planet's equatorial plane for a given V_∞ with respect to the moon. A geometric argument to support this statement is offered by Uphoff [13]. The application in [13] involves the Galilean satellites of Jupiter and assumes that the natural satellite is in a circular orbit with zero inclination. Uphoff's result is modified for the Saturn-Titan system and the moon Titan is allowed a non-zero flight path angle, although a zero inclination for Titan is still assumed. Under these conditions, the maximum inclination achieved via a Titan flyby at the spacecraft orbit periapsis is

$$\cos\left(i_{max}\right) = \frac{\left(X^2 - \sin^2\gamma_T\right)^{1/2}}{\cos\gamma_T} \tag{3}$$

where γ_T refers to Titan's flight path angle and

$$X = \frac{\left(V^2 + V_T^2 - V_\infty^2\right)}{2VV_T} \tag{4}$$

In Equation (4), V is the magnitude of the velocity of the spacecraft, V_T is Titan's velocity with respect to Saturn, and V_∞ is the velocity of the spacecraft with respect to Titan. If $\gamma_T = 0$, the resulting expression for the maximum inclination is equal to that in Uphoff.

To achieve the optimal orbit geometry for a minimal ΔV cost, using Titan flybys to drive $r_{p,old}$ to its maximum value before implementing a maneuver is equivalent to maximizing the inclination of the orbit to the value i_{max} as determined from Equation (3). Assuming that the periapse-raise maneuver occurs at apoapsis in an orbit meeting these requirements, the optimal cost is plotted in Fig. 1. The figure includes plots of periapse-raise costs associated with orbits of various periods meeting these criteria. The numbers in brackets represent resonances between the period of the spacecraft orbit and the period of Titan in the patched-conic model. For example, a maneuver of 100 m/s (the red line in the figure) can raise the periapsis of a 160-day orbit (inclined at $i_{max} = 47^o$) to 25.6 R_S. For different values of V_∞, the plot in Fig. 1 will change but the values still represent good approximations.

The target periapse values in Fig. 1 are derived from conic analysis. In a higher fidelity model, the periapse distances can vary due to the perturbations of other attracting bodies such as the Sun and Titan. However, it is generally expected and confirmed in Fig. 1, that the same target periapsis can be achieved with a smaller ΔV on a larger orbit. The time penalty for a maneuver at apoapsis (half an orbit period after the last Titan flyby) is also larger for the longer orbital period.

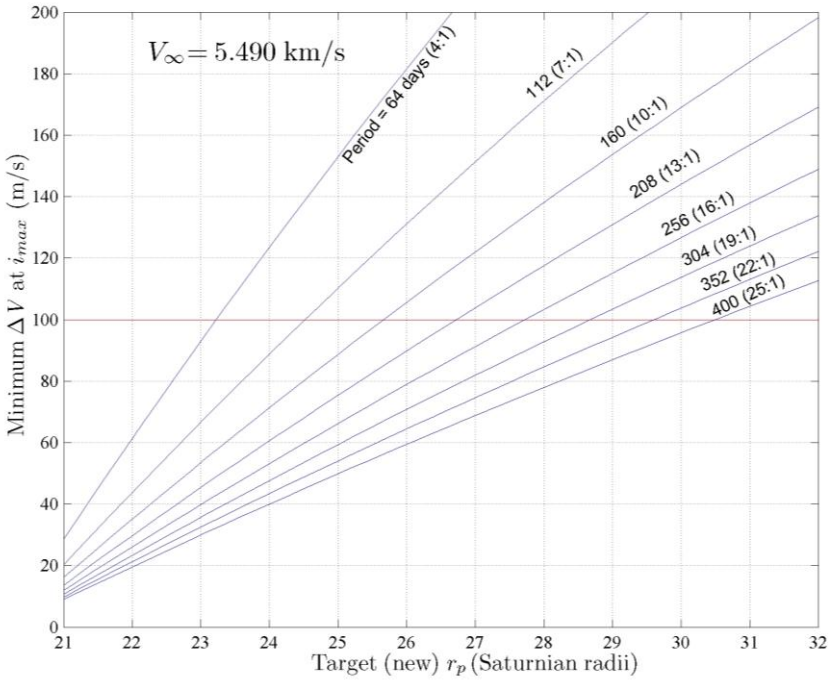

Figure 1. Optimal maneuver cost for periapse raise at maximum inclination (i_{max}).

ANALYSIS AND RESULTS

Strategy to Compute a Long-Term Trajectory in the Ephemeris Model

The steps in the following example represent a design strategy to produce a deterministic trajectory that meets the desired objectives. From an initial conic design that possesses the desired orbital characteristics, a model is incorporated including multiple gravity fields and the orbital characteristics are maintained throughout a 500-year simulation.

Consider a scenario that exploits Titan flybys to insert the spacecraft into an orbit inclined at nearly 50^{o} relative to Saturn's equatorial plane. Assume that V_{∞} relative to Titan is originally equal to 5.887 km/s. The preliminary design is accomplished via the satellite tour design program STOUR, a software tool that was developed at the Jet Propulsion Laboratory for the Galileo mission tour design [14]. This program has been enhanced and extended at Purdue University to enable the automated design of gravity-assist tours in the solar system as well as the satellite system of Jupiter [15-18]. STOUR derives states of planets and moons from ephemeris information and uses a patched-conic model to calculate gravity-assist trajectories meeting specified requirements. STOUR is used to deliver the spacecraft to the appropriate final Titan encounter by working to achieve the maximum inclination that will simultaneously achieve the maximum periapse radius. Given a satisfactory tour design and acceptable final Titan flyby, the orbit is propagated in a conic model to a point that is 10 days past the Titan encounter. The corresponding ephemeris states of Saturn, Titan, and the Sun, along with the spacecraft state, constitute a set of initial conditions to be passed to a more comprehensive model that more accurately predicts the apoapse state of the spacecraft. At apoapse arrival, the periapse-raise maneuver is added and the propagation proceeds with a long-term integrator in a higher fidelity model including gravity and the full ephemeris states of the Sun, Saturn, Titan, and Jupiter. Since the baseline orbit extends out to a region occupied by Hyperion, Iapetus, and Phoebe, these moons are also included in the long-term propagation. The steps are represented in Fig. 2 for a specific example. From the final Titan flyby, an orbit with a period of 160 days (10:1 Titan resonance in a conic sense) is selected as a baseline and a target radius of 25 R_S is defined as the new periapsis since this distance is significantly higher than Titan's orbit and can be achieved with a nominal cost around 100 m/s according to the plot in Fig. 1. Though the departure orbit possesses a 10:1 resonance with Titan, the resonance cannot be exactly maintained for the long term after

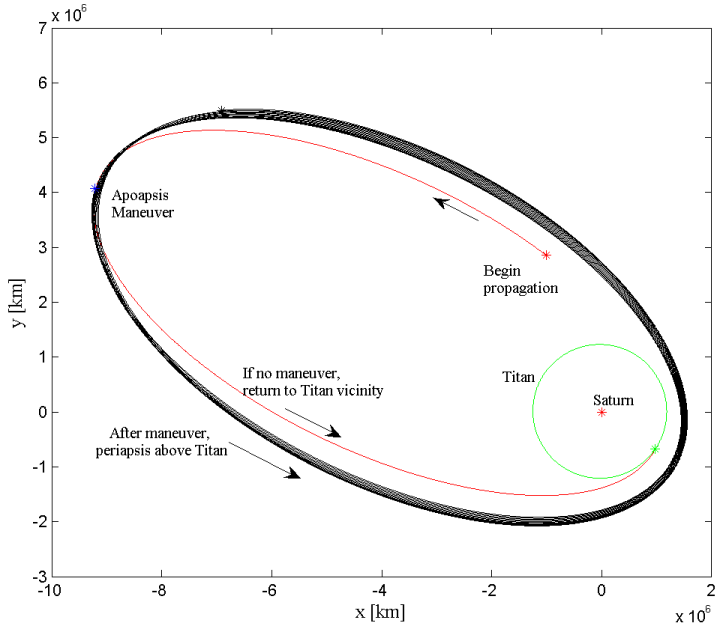

Figure 2. Steps to produce an orbit with r_p beyond the orbit of Titan; final simulation incorporates full ephemeris data.

the maneuver. It is noted that a periapse raise is usually less costly in a larger orbit with a more distant apoapsis, however, such large orbits are subjected to larger variations in their periapsis over time due to gravitational perturbations and are, thus, more likely to reencounter Titan.

Long-Term Effects of Gravity Perturbations on Periapse Variations

As long as no close encounter with a moon occurs, the semimajor axis of the orbit does not undergo significant secular variation; thus, long-term variations in periapse distance are due largely to changes in eccentricity. The plots in Fig. 3 reflect osculating eccentricity values over a 500-year span for the baseline orbit. In the figure, several eccentricity curves appear as different sets of bodies are incorporated into the gravity model. With only Saturn in the model, the orbit is a perfect conic and the eccentricity is constant, as expected. Once the Sun is included in the model, the most significant variations over 500 years are apparent. The variations after adding Jupiter, Titan, and the other moons are apparently less significant. No flybys of Titan occur after the initial periapse-raise maneuver, thus the orbital energy and semimajor axis do not change significantly and it is anticipated that periapse variations will mirror eccentricity variations. The plot of periapse variations in Fig. 4 demonstrates that this, in fact, is true. Also note the red line in Fig. 4 indicating the apoapse distance of Titan.

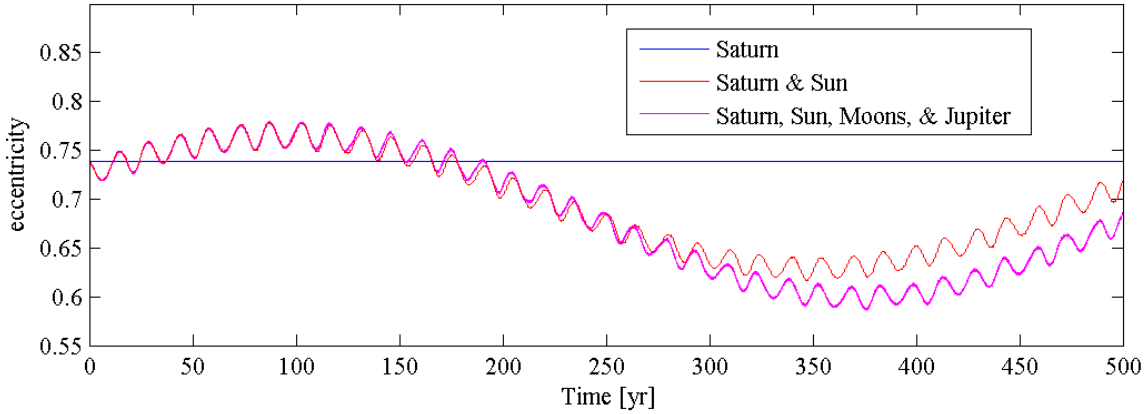

Figure 3. Eccentricity variations over time using different force models.

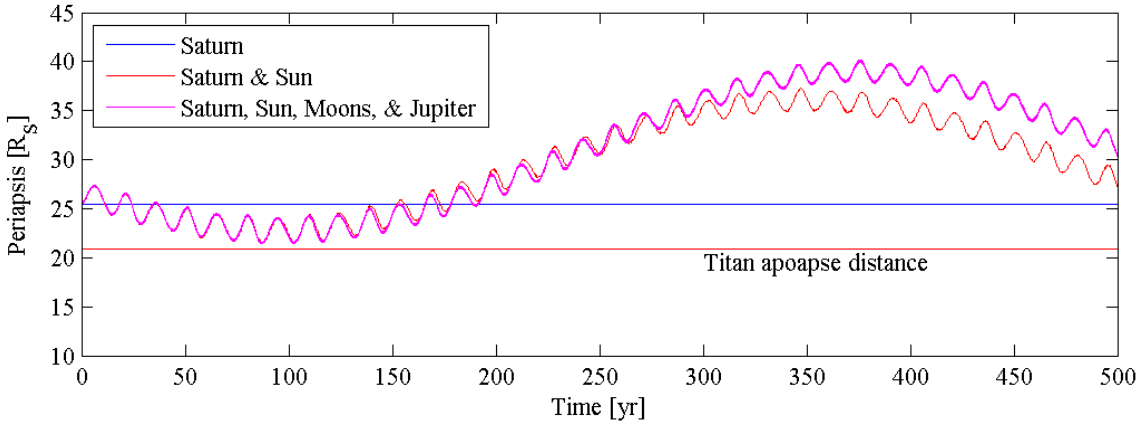

Figure 4. Periapsis variations reflect the eccentricity variations. Addition of the solar gravity perturbation has the largest effect. The red line indicates Titan's apoapsis.

The solar perturbations cause variations in eccentricity and periapse radius that are composed of several periodic or quasi-periodic terms. There are three such terms, in particular, that are apparent upon visual inspection of the figures. The first term possesses a period equal to that of the spacecraft orbit, 167

days; the amplitude of this variation is too small to be identified at the scale of the plots in Figs. 3 and 4. The period corresponding to the second term is approximately 15 years, which is one half that of Saturn's orbit around the Sun. This short-period term is readily apparent in the figure. The third term is associated with the largest amplitude and an apparent period of just over 500 years.

The significance of any variation that is based on Saturn's orbital period may be most clearly interpreted from the perspective of a Sun-Saturn rotating frame. Such a frame is defined in Fig. 5. The $\hat{x}-$axis is directed from the Sun toward Saturn. The $\hat{y}-$axis is perpendicular to the $\hat{x}-$axis and in the plane of Saturn's orbit, positive in the general direction of Saturn's velocity. The figure also subdivides the space around Saturn into four quadrants in the $\hat{x}-\hat{y}$ plane. These are defined counterclockwise as indicated, with quadrant I on the far side of Saturn from the Sun and leading Saturn's orbit. Orientation within each quadrant is defined in terms of an angle relative to the Sun-Saturn line, as indicated in the figure. The impact of the solar gravity perturbation on the orbit differs depending on the quadrant [5]. For the eccentricity variations, orbits with apoapsis in quadrants I and III elongate signaling an increase in eccentricity, while the eccentricity of orbits with apoapsis in quadrants II and IV decreases. Recall that one of the variations in Fig. 3 possesses a period of approximately 15 years, roughly half the period of Saturn. This variation is produced by the solar perturbation effects acting on the orbit as apoapsis rotates through the four quadrants in the Sun-Saturn rotating frame.

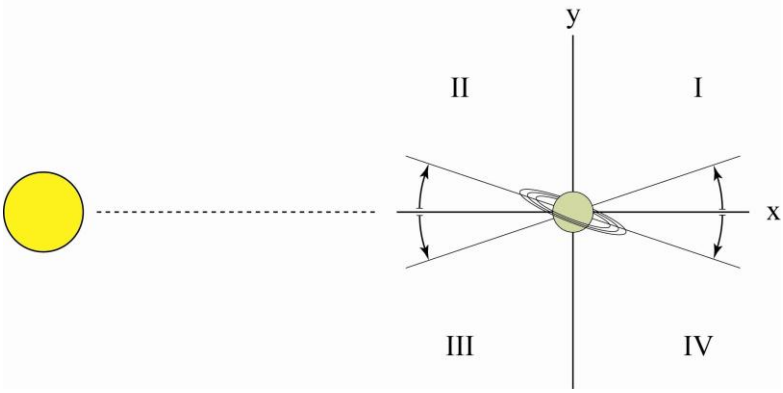

Figure 5. Orientation angle in each quadrant as defined in the rotating frame [7].

Impact of Initial Orbit Orientation on the Long-Term Variations

To demonstrate the link between quadrants and eccentricity variations, the baseline orbit is propagated for a short time using a model associated with the Sun-Saturn circular restricted three-body problem (CR3BP). The CR3BP assumes that only the Sun and Saturn act gravitationally on the spacecraft and that Saturn is in a circular orbit about the Sun. This model is used for a lower fidelity analyses when the gravitational perturbation of the Sun is the dominant perturbing force. Recall that Figs. 3 and 4 indicate that the solar perturbation represents the largest effect on eccentricity and periapse radius. Results from analyses in the CR3BP are often transitioned to higher fidelity models including multiple bodies.

The baseline orbit propagation in the CR3BP appears in Fig. 6a, plotted in the rotating frame and centered at Saturn. This trajectory originates with apoapsis in quadrant IV but near to the Sun-Saturn line (the $\hat{x}-$axis). Due to the frame rotation, the orbit cycles clockwise in the figure from quadrant IV to quadrant III and eventually to quadrant I. In one half of this cycle, the orbit will pass through a quadrant where eccentricity decreases (quadrant II or IV in red) followed by a quadrant where eccentricity increases (quadrant I or III in blue). A plot of eccentricity as a function of time as apoapsis passes through the quadrants appears in Fig. 6b. Due to the cycling of the orbit through the quadrants, the value of eccentricity varies with a period equal to one half the cycle time. One full cycle is completed in roughly one period of Saturn's orbit, nearly 30 years, thus, this variation has a period of roughly 15 years.

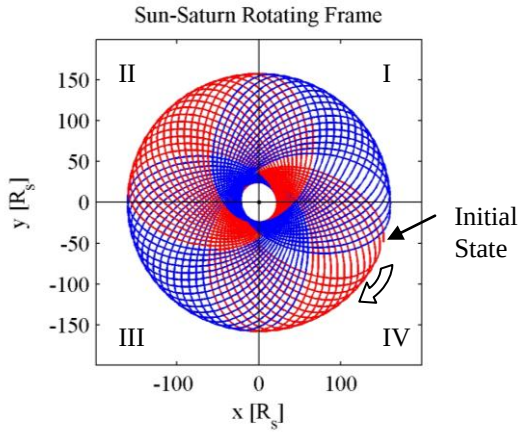

Figure 6a. Propagation of a baseline orbit about Saturn in the CR3BP; Saturn-centered.

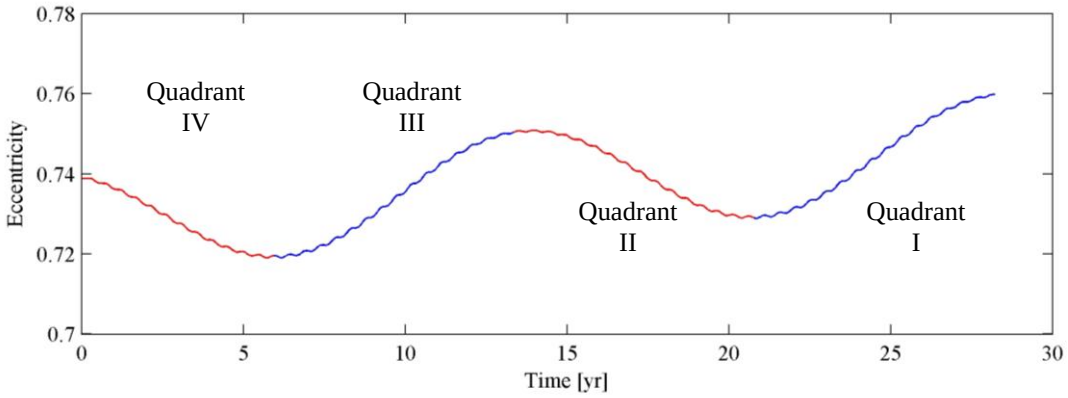

Figure 6b. A 15-year variation in eccentricity is correlated with the orbit apoapsis cycling through two quadrants in 15 years.

At the initiation of the propagation, the location of apoapsis within a specific quadrant will determine the initial phase corresponding to the curves representing the variations. As demonstrated in Fig. 7a and Fig. 7b, the long-term impact of the initial phase on eccentricity and periapse distance is apparent. The propagations in Fig. 7 are initiated with the baseline initial conditions after a periapsis-raise maneuver along the 10:1 resonance orbit (the same baseline conditions used for Fig. 6). The red line results from propagation in a circular restricted three-body model where the Sun and Saturn are confined to circular orbits about their barycenter. The black curve reflects the same propagation in an ephemeris model including the Sun and Saturn. No significant difference in the large scale variations due to solar gravity exists between the two models. Observe that there are periodic peaks and troughs in the periapse curves (Fig. 7b). The baseline initial conditions, in red, possess an apoapsis in quadrant IV, but only 17^o from the $\hat{x}-$axis. When these initial conditions are rotated 180^o to quadrant II, they produce exactly the same variations in eccentricity over time. Thus, the red curve results from propagation of initial conditions in both quadrant II and quadrant IV, originating near the $\hat{x}-$axis. The propagation that yields the magenta curve possesses initial conditions in quadrants I and III but near the $\hat{y}-$axis. Associated with this cure, the minimum r_p distance dips below the apoapse distance corresponding to Titan's orbit (indicated by a flat red line). It is desirable to avoid an r_p below the orbit of Titan such that an encounter with Titan is less probable. The apoapsis of the initial orbit associated with the green curve is 45^o from the $\hat{x}-$axis in quadrant IV. From this analysis it is apparent that the initial quadrant for the orbit apoapsis will determine the phase of the 15-year variation, and the specific pattern of peaks and troughs. In particular, initial conditions nearer to the $\hat{x}-$axis (with a smaller quadrant angle) will correspond to a trough in the periapsis

variations, a peak in eccentricity, and subsequent propagation yields an immediate rise in the periapsis distance. In contrast, the orbits originating near the $\hat{y}-$axis in the rotating frame are initializing in a peak in the periapsis variations and generally develop lower periapse distances over time. These periapses cross Titan's orbit in this example, indicating a stronger likelihood of Titan encounters. Thus, initial conditions with apoapses near the $\hat{x}-$axis of the Sun-Saturn rotating frame are good candidates for generating orbits that will not reencounter Titan; they generally maintain a higher periapsis over time.

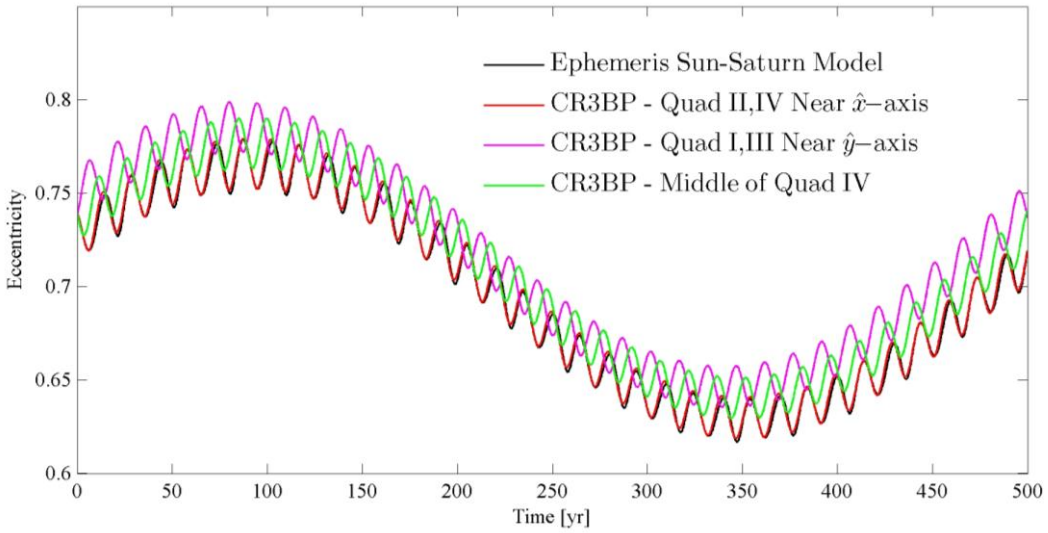

Figure 7a. Eccentricity variations for simulations that originate in different quadrants.

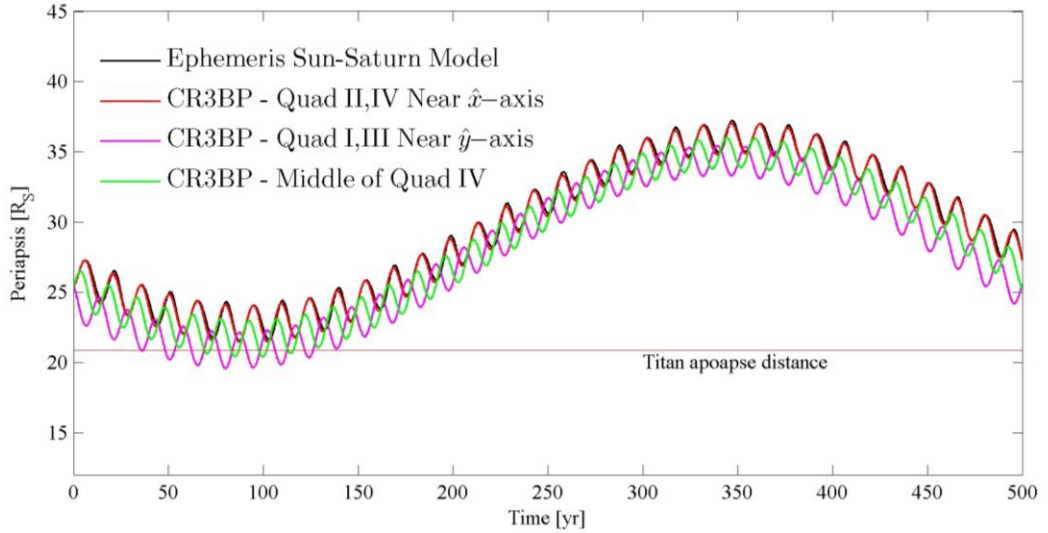

Figure 7b. Periapsis variations for simulations that originate in different quadrants.

Long-Term Impact of Inclination

The amplitude of the long-period term in the Sun-Saturn model is largely dependant on the inclination of the spacecraft orbit with respect to the Sun-Saturn orbital plane. This is demonstrated in Fig. 8. The first propagation, plotted with a black curve, incorporates the exact ephemeris locations of the Sun and Saturn; the second simulation, plotted in red, is accomplished in the CR3BP. The two curves are virtually indistinguishable, confirming again that the CR3BP serves as a sufficient model for further analysis of the

solar perturbations. The baseline orbit, when transformed to the Sun-Saturn rotating frame, possesses an inclination of approximately 30^o relative to the plane of Saturn's orbit. The initial state is altered to produce two similar orbits with different inclinations. With an inclination of 20^o, the magnitude of the long term variation is clearly lowered. With an inclination of 0^o with respect to the Sun-Saturn plane, the long-term variation is not observed at all. This result is consistent with an understanding of the impact of solar perturbations on changes in inclination.

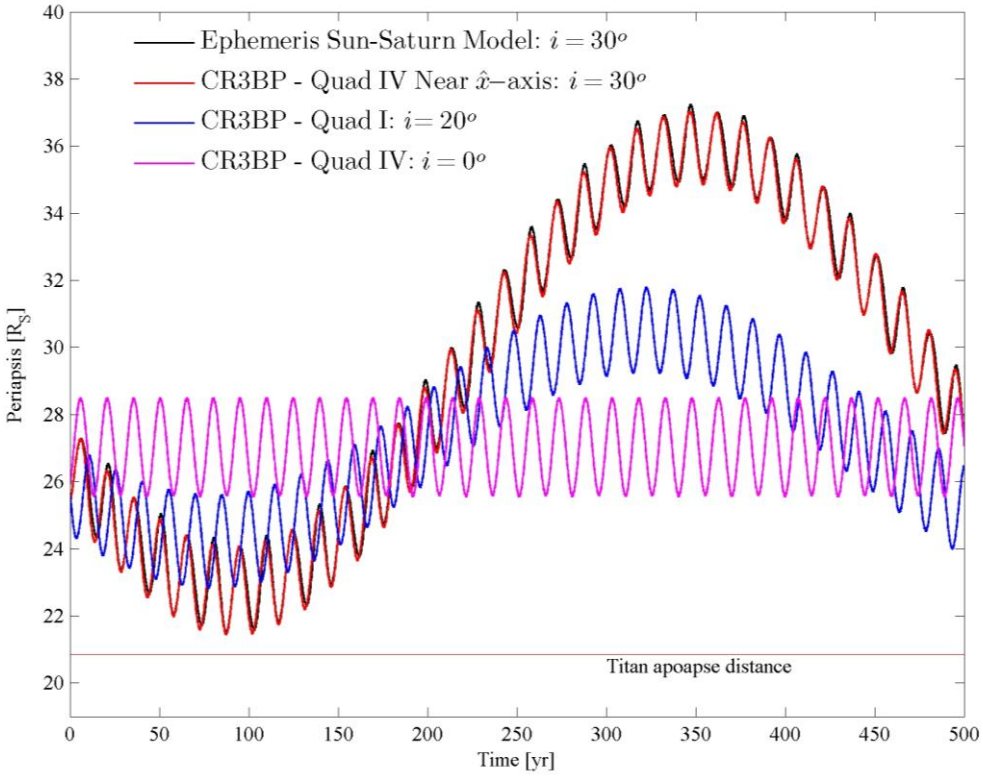

Figure 8. Periapsis variations at smaller inclinations demonstrate smaller amplitudes in the long term variation.

There are, then, two competing observations for orbit inclination. To achieve the most efficient periapse-raise maneuver, the inclination with respect to the Saturn equator must be maximized to around 50^o. Yet, to minimize large-amplitude long-term variations in periapse distance with the intention of preventing a future Titan encounter, the inclination with respect to the ecliptic plane should be as low as possible. The two planes of reference in these geometric requirements differ by 26.7^o. One solution for this problem is to time the final Titan encounter (simultaneously, the spacecraft orbit periapsis) prior to the periapse-raise maneuver such that Titan is on the line of intersection between the ecliptic and the equatorial planes. Similarly, the spacecraft orbit line of nodes is along the intersection of the planes. In this configuration, an inclination of $i_1 = 50^o$ with respect to the equatorial plane is equivalent to an inclination of $i_2 = i_1 - 26.7^o = 23.3^o$ with respect to the ecliptic. According to the analysis in the CR3BP, such a low inclination will result in long-term variations of smaller magnitude. Of course, specification of the orbit plane such that the descending node is aligned with the intersections of ecliptic and equatorial planes precludes any freedom in the placement of apoapsis. The plane intersection determines the quadrant as well as the orientation within the quadrant. Thus, the choice of initial phasing in the 15-year period variations is limited when attempting to lower the amplitude in the long-term variations.

Results

To demonstrate the design steps, a particular example is examined in detail. A trajectory is generated by STOUR based on a possible end-state associated with the extended mission (a 16-day orbit with a Titan V_∞ of 5.5 km/s). The subsequent design can be accomplished in three main phases. (i) The first phase uses a series of non-resonant transfers (in the equatorial plane) to rotate the Titan encounter location and fix the right ascension of the ascending node (Ω). (ii) The second phase maintains a 16-day orbit, but cranks up the inclination to its maximum value, raising periapsis to its maximum value as well. (iii) The third phase incorporates additional Titan flybys and pumps up the orbital period (to 160, 304, or 400 days) for a periapse-raise maneuver. This sequence of steps requires ~640 days and 23 Titan flybys. Before the periapse-raise maneuver can be implemented, an additional time interval equal to one half the period of the final orbit is necessary to reach apoapsis.

The process generates three sample scenarios for the final trajectory depending on the post-encounter conditions from the final Titan flyby. The 160-day orbit is defined by a 10:1 conic resonance with Titan and requires 80 days post-encounter to transfer to apoapsis before the maneuver. The 304-day orbit results from a 19:1 conic resonance with Titan and requires a time-of-flight to apoapsis of 152 days. Finally, a 25:1 conic resonance with Titan yields a 400-day spacecraft orbit, such that 201 days are required to reach apoapsis. Propagations to apoapsis include the gravity of both the Sun and Titan. At apoapsis of each orbit, a 100 m/s maneuver is added. This is more than sufficient in a conic model to raise periapsis above 25 R_S. (See Fig. 2) As mentioned, this strategy lowers the inclination of the spacecraft orbit with respect to the Saturn orbital plane but does not design for placement of apoapsis within any particular quadrant. In these three cases, apoapses lie roughly in the middle of quadrant II between 40^o and 50^o with respect to the $\hat{x}-$axis.

The history of the periapse distance, as a function of time, for each of the three examples is plotted in Fig. 9. The differential equations are propagated for 500 years in the high fidelity model including the gravity perturbations of the Sun, Jupiter, Titan, Hyperion, Iapetus, and Phoebe; the location of each body is obtained from ephemeris data. Recall as previously mentioned that larger orbits with longer periods (higher r_a values) result in more significant periapsis variations. Yet, the main characteristics of the curves remain the same in all cases – i.e., the three apparently most significant quasi-periodic terms, of different amplitudes and periods. The curves (green and magenta) for the periapses of the 400-day and 303-day orbits now possess amplitudes that are sufficiently large to expose the smallest variation that can be observed at this scale. It is also observed that the long period decreases as the size of the orbit increases. From about 500 years for the 160-day orbit to approximately 150 years for the 400-day orbit, this shift reflects the increase in the long term frequency associated with inclination rate of change. All three trajectories remain beyond the apoapse radius of Titan.

The trajectory propagated from the 10:1 conic resonance orbit is plotted again in Fig. 10 along with the orbits of Titan, Hyperion, Iapetus, and Phoebe. The closest approach between the spacecraft and each of the four moons is listed in Table 1. It is notable that in the first example, the spacecraft never passes closer than a million kilometers to Titan over 500 years. At the time when the maneuver is added at the spacecraft apoapsis, Titan and the spacecraft are in a 10:1 conic resonance and are in-phase such that another encounter occurs without the maneuver. Due to the maneuver at apoapsis, however, the period of the spacecraft orbit is increased and a near 21:2 conic resonance with Titan is achieved, i.e., the spacecraft period is increased by a value equal to one-half the period of Titan. One spacecraft period is then 10.5 Titan periods and, thus, in the time the spacecraft returns to periapsis from apoapsis, Titan moves through 5.25 revolutions, placing Titan one quarter revolution out-of-phase with the spacecraft. Consider Fig. 11, a view relative to the Sun-Saturn frame and centered at Saturn. The locations of periapsis passage of the spacecraft (in blue) along with the position of Titan at the corresponding times (in red) are plotted. As the spacecraft crosses Titan's orbit, Titan itself is in a different location along its path so that the two bodies are always out-of-phase and do not encounter each other. Achieving this out-of-phase resonance is another mechanism to avoid reencounters with Titan. Since no encounters with Saturn's moons occur to significantly alter the spacecraft's orbital energy, its period remains relatively constant over the 500-year

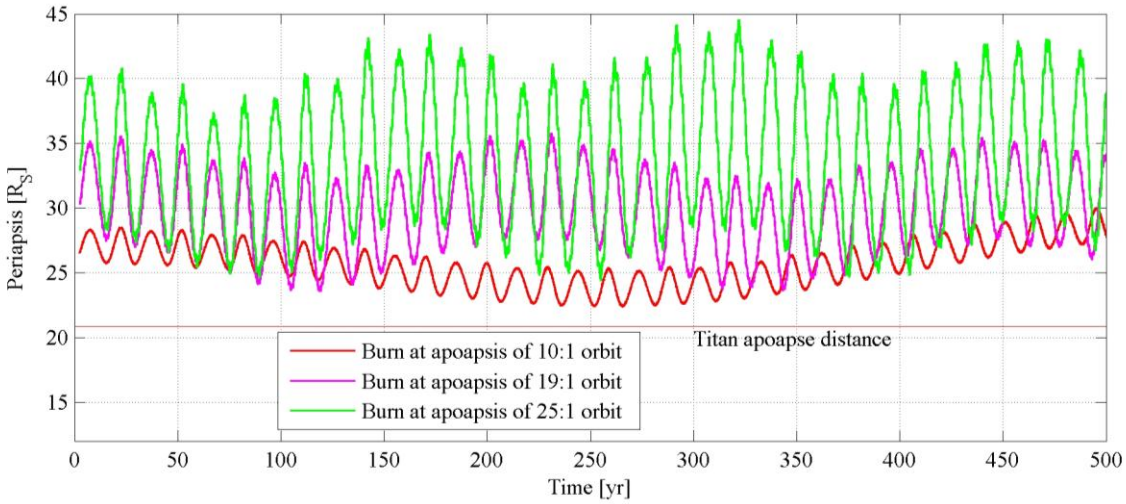

Figure 9. Periapsis variations over time for the sample cases.
All periapses remain beyond Titan (red line at 20.2 R_S).

propagation. In Fig. 12, it is apparent that the osculating period does not vary by more than 1.5 days. Thus, the out-of-phase resonance with Titan is maintained naturally. Titan is always approximately one-quarter revolution away from the spacecraft as the spacecraft reaches periapsis.

The spacecraft orbit does appear to cross the orbit of Iapetus in the planar view in Fig. 10. However, given the orbit inclination history, it is apparent that the plane of the spacecraft orbit changes significantly over 500 years. Thus, there are only two relatively brief intervals over that time span when the spacecraft and Iapetus pass roughly 100,000 km apart (as noted in Table 1).

Table 1. Closest approach to moons of Saturn [km]

Body	160-day orbit (10:1)	303-day orbit (19:1)	400-day orbit (25:1)
Titan	**1,131,110**	**277, 001**	**422,745**
Hyperion	**31,478**	**155,102**	**143,330**
Iapetus	**118,038**	**79,718**	**91,988**
Phoebe	**2,573,332**	**302,830**	**67,962**

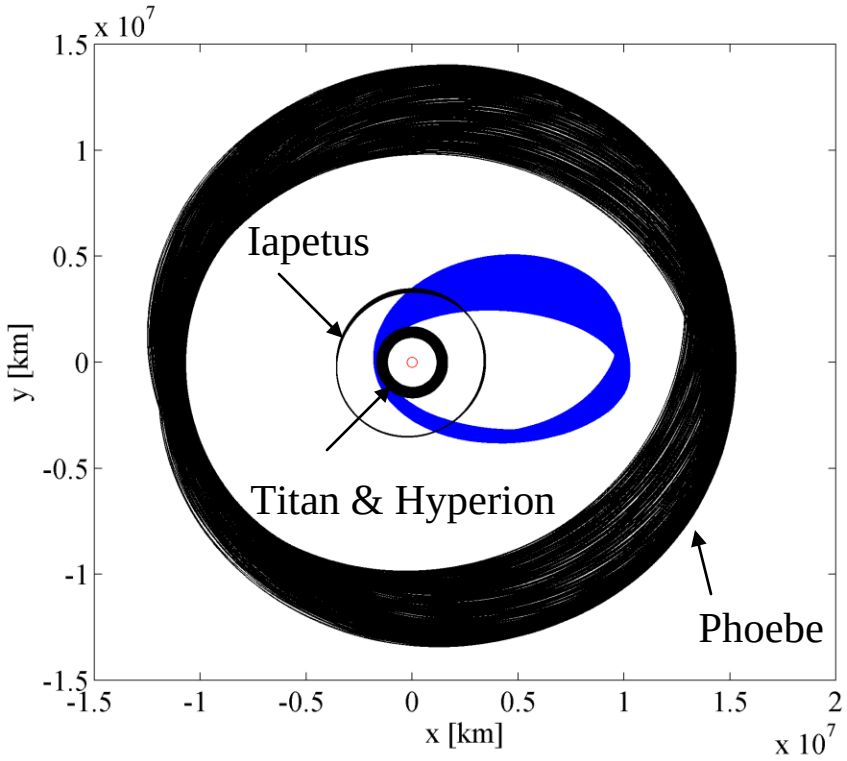

Figure 10 Propagation of the 10:1 resonance orbit for 500 years. Saturn-centered; spacecraft path in blue.

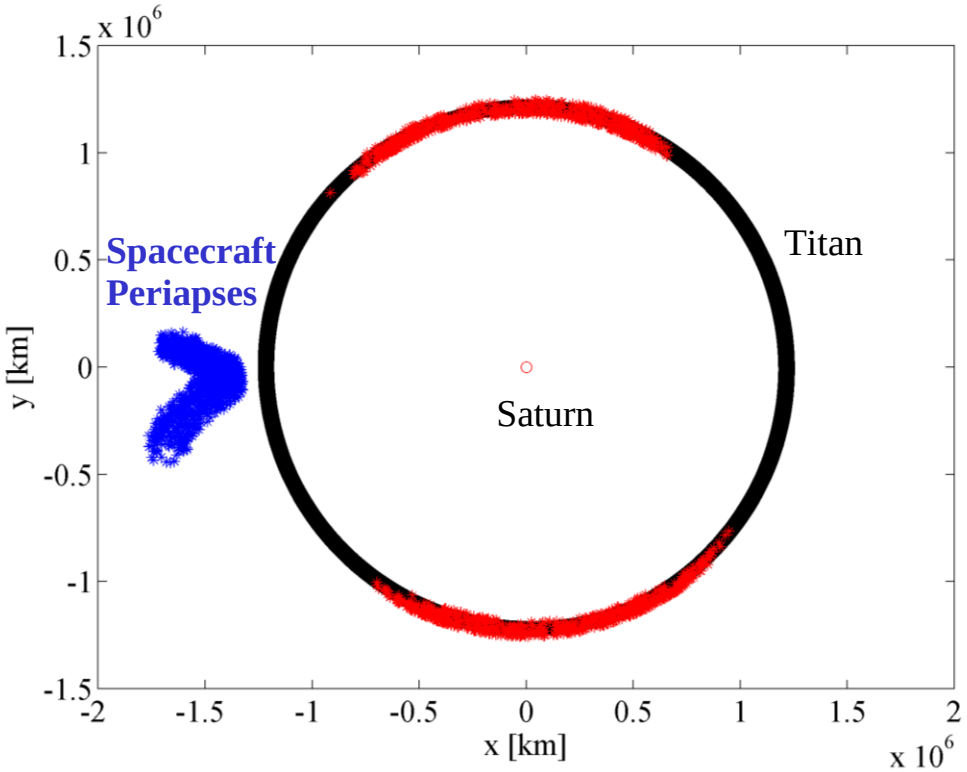

Figure 11 Periapses states along the 10:1 resonant orbit during a 500-year high fidelity propagation; red indicates Titan's location at the time of spacecraft periapsis passage.

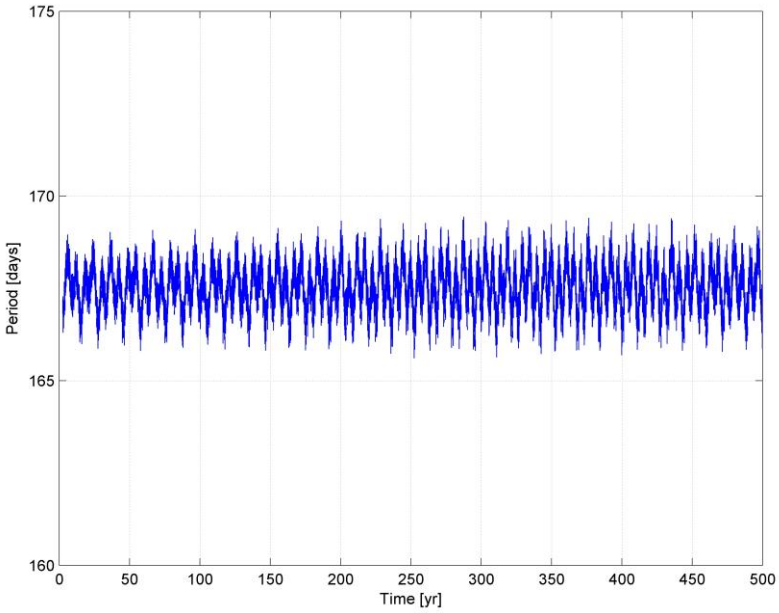

Figure 12 Osculating period after maneuver.

CONCLUDING REMARKS

A large, eccentric orbit about Saturn, between the orbits of Titan and Phoebe, is considered as an end-of-life option for the Cassini spacecraft. Orbits of this type can be achieved via Titan encounters with a maneuver less than 100 m/s. Orbital perturbations due to the gravitational influences of other bodies can be significant but do not prohibit a 500-year orbit without impacting Titan or the other moons. A desirable orbit can be identified assuming that appropriate quadrant orientation and baseline inclination are achieved.

ACKNOWLEDGEMENTS

The authors would like to thank Diane Craig Davis for her assistance. Valuable discussions with Nathan J. Strange and Jerry B. Jones (Technical Manager) are appreciated. Portions of this work were supported by Purdue University and the Jet Propulsion Laboratory, California Institute of Technology, under contract number 1283234 with the National Aeronautics and Space Administration.

REFERENCES

[1] Pioneer Mission [http://www.nasa.gov/mission_pages/pioneer/].

[2] Voyager, The Interstellar Mission [http://voyager.jpl.nasa.gov/index.html].

[3] Bindschadler, D. L., Theilig, E. E., Schimmels, K. A., and Vandermey, H., "Project Galileo: Final Mission Status," 54th International Astronautical Congress of the International Astronautical Federation, International Academy of Astronautics and International Institute of Space Law, Bremen, Germany, September 29th, 2003.

[4] National Space Science Data Center [nssdc.gsfc.nasa.gov/database/MasterCatalog?sc=1971-051A].

[5] Viking Mission [www.nasa.gov/mission_pages/viking].

[6] Yam, C. H., Craig Davis, D., Longuski, J. M., and Howell, K. C., "Saturn Impact Trajectories for Cassini End-of-Life," AAS/AIAA Astrodynamics Specialist Conference, Mackinac Island, Michigan, August 20-23, 2007.

[7] Craig Davis, D., Patterson, C., and Howell, K., "Solar Gravity Perturbations to Facilitate Long-Term Orbits: Application to Cassini," AAS/AIAA Astrodynamics Specialist Conference, Mackinac Island, Michigan, August 20-23, 2007.

[8] Okutsu, M., Yam, C. H., Longuski, J. M., and Strange, N. J., "Cassini End-of-Life Escape Trajectories to the Outer Planets," AAS/AIAA Astrodynamics Specialist Conference, Mackinac Island, Michigan, August 20-23, 2007.

[9] Szebehely, V., *Theory of Orbits: The Restricted Problem of Three Bodies*. New York: Academic Press, 1967.

[10] Sheppard, Scott S., "Outer Irregular Satellites of the Planets and Their Relationship with Asteroids, Comets, and Kuiper Belt Objects," IAU Symposium No. 229, May 2006.

[11] Hamilton, D. P., and Krivov, A. V., "Dynamics of Distant Moons of Asteroids," *Icarus* Vol. 128, 1997, pp. 241-249.

[12] Carruba, V., Burns, J. A., Nicholson, P. D., and Gladman, B. J., "On the Inclination Distribution of the Jovian Irregular Satellites," *Icarus* Vol. 158, 2002, pp. 434-449.

[13] Uphoff, C., Roberts, P.H., and Friedman, L.D., "Orbit Design Concepts for Jupiter Orbiter Missions," *Journal of Spacecraft and Rockets*, Vol. 13, No. 6, 1976, pp. 348-355.

[14] Rinderle, E. A., "Galileo User's Guide, Mission Design System, Satellite Tour Analysis and Design Subsystem," Jet Propulsion Laboratory Report JPL D-263, California Institute Of Technology, Pasadena, California, July 1986.

[15] Williams, S. N., "Automated Design of Multiple Encounter Gravity-Assist Trajectories," M.S. Thesis, School of Aeronautics and Astronautics, Purdue University, West Lafayette, Indiana, August 1990.

[16] Longuski, J. M., and Williams, S. N., "Automated Design of Gravity-Assist Trajectories to Mars and the Outer Planets," *Celestial Mechanics and Dynamical Astronomy*, Vol, 52, No. 3, 1991, pp. 207-220.

[17] Patel, M. R., "Automated Design of Delta-V Gravity-Assist Trajectories for Solar System Exploration," M. S. Thesis, School of Aeronautics and Astronautics, Purdue University, West Lafayette, Indiana, August 1993.

[18] Bonfiglio, E. P., "Automated Design of Gravity-Assist and Aerogravity-Assist Trajectories," M. S. Thesis, School of Aeronautics and Astronautics, Purdue University, West Lafayette, Indiana, August 1999.